Contribution of hydroxymethanesulfonate (HMS) to severe winter haze in the North China Plain

Tao Ma[1], Hiroshi Furutani[2,3], Fengkui Duan[1], Takashi Kimoto[4], Jingkun Jiang[1], Qiang Zhang[5], Xiaobin Xu[6], Ying Wang[6], Jian Gao[7], Guannan Geng[1], Meng Li[5], Shaojie Song[8], Yongliang Ma[1], Fei Che[7], Jie Wang[7], Lidan Zhu[1], Tao Huang[4], Michisato Toyoda[3], Kebin He[1]

[1]State Key Joint Laboratory of Environment Simulation and Pollution Control, School of Environment, State Environmental Protection Key Laboratory of Sources and Control of Air Pollution Complex, Beijing Key Laboratory of Indoor Air Quality Evaluation and Control, Tsinghua University, Beijing 100084, China
[2]Support Center for Scientific Instrument Renovation and Custom Fabrication, Osaka University, Osaka, 560-0043, Japan
[3]Project Research Center for Fundamental Sciences, Graduate School of Science, Osaka University, Osaka, 560-0043, Japan
[4]Kimoto Electric Co., Ltd, 3-1 Funahashi-cho Tennoji-ku, Osaka 543-0024, Japan
[5]Ministry of Education Key Laboratory for Earth System Modeling, Department of Earth System Science, Tsinghua University, Beijing 100084, China
[6]State Key Laboratory of Severe Weather & Key Laboratory for Atmospheric Chemistry of CMA, Chinese Academy of Meteorological Sciences, Beijing 100081, China
[7]State Key Laboratory of Environmental Criteria and Risk Assessment, Chinese Research Academy of Environmental Sciences, Beijing 100012, China
[8]School of Engineering and Applied Sciences, Harvard University, Cambridge, MA 02138, USA

Correspondence to: Fengkui Duan (duanfk@mail.tsinghua.edu.cn) and Kebin He (hekb@tsinghua.edu.cn)

Abstract. Severe winter hazes accompanied by high concentrations of fine particulate matter ($PM_{2.5}$) occur frequently in the North China Plain and threaten public health. Organic matter (OM) and sulfate are recognized as major components of $PM_{2.5}$, while atmospheric models often fail to predict their high concentrations during severe winter hazes due to incomplete understanding of secondary aerosol formation mechanisms. By using a novel combination of single particle mass spectrometer and optimized ion chromatography measurement, here we show that hydroxymethanesulfonate (HMS), formed by the reaction between formaldehyde (HCHO) and dissolved SO_2 in aerosol water, is ubiquitous in Beijing winter. The HMS concentration and the molar ratio of HMS to sulfate increased with the deterioration of winter haze. High concentrations of precursors (SO_2 and HCHO) coupled with low oxidant levels, low temperature, high relative humidity, and moderately acid pH facilitate the heterogeneous formation of HMS, which could account for up to 15% of OM in winter haze and lead to 36% overestimates of sulfate when using traditional ion chromatography measurements. Despite the clean air actions have substantially reduced SO_2 emissions, HMS concentration and molar ratio of HMS to sulfate during severe winter hazes increased from 2015 to 2016 with the growth of HCHO concentration. Our findings illustrate the significant contribution of heterogeneous HMS chemistry to severe winter hazes in Beijing, which help to improve the prediction of OM and sulfate, and suggest that the reduction in HCHO can help to mitigate haze pollution.

1 Introduction

35 Severe winter haze pollution with high $PM_{2.5}$ (particles with aerodynamic diameter ≤ 2.5 μm) concentration occurs frequently in the North China Plain (NCP), exerting adverse impacts on the environment and human health (Huang et al., 2014; Lelieveld et al., 2015). Secondary components, constituting a large fraction of $PM_{2.5}$, are key drivers of haze formation (Huang et al., 2014), however, atmospheric models with known formation mechanisms often fail to predict high levels of secondary organic matter (OM) and sulfate during severe winter hazes.

40 Traditional models with gas-phase photochemical mechanisms and aqueous chemistry involving glyoxal and methylglyoxal significantly underestimate the high OM levels observed in NCP winter (Wang et al., 2014; Zheng et al., 2015a). Adding heterogeneous reactions involving isoprene epoxide, glyoxal, and methylglyoxal, and accounting for organic aerosol aging and oxidation of intermediate-volatility organic compounds can improve the model predictions of OM (Hu et al., 2017; Zhao et al., 2016; Yang et al., 2018), however, high OM concentrations observed in Beijing winter are still underpredicted (Hu et

45 al., 2017), especially during the periods with low oxidant concentrations and weak photochemical activity.

In addition to OM, high levels of particulate sulfate are often observed in NCP winter and it increases sharply with increasing $PM_{2.5}$ pollution levels (Zheng et al., 2015b). Traditional atmospheric models containing both gas-phase oxidation of SO_2 by OH radicals and aqueous-phase reaction pathways involving H_2O_2, O_3, and O_2 catalyzed by Fe^{3+} and Mn^{2+} fail to reproduce the observed high sulfate levels, and revised models with heterogeneous chemistry greatly improve the sulfate simulation

50 (Wang et al., 2014; Zheng et al., 2015a). Cheng et al. and Wang et al. reported that the oxidation of SO_2 by NO_2 in aerosol water under high pH could explain the difference between modeled and observed sulfate (Cheng et al., 2016; Wang et al., 2016). On the other hand, the misidentification of organosulfur compounds as inorganic sulfate in conventional measurements can lead to overestimation in the observed particulate sulfate (Chen et al., 2019). Recently, Moch et al. and Song et al. reported the potential contribution of hydroxymethanesulfonate (HMS, $HOCH_2SO_3^-$) to particulate sulfur during winter haze in Beijing

55 (Moch et al., 2018; Song et al., 2019). However, there is no direct evidence for the content of HMS in haze particles, and the formation mechanism of HMS in NCP winter hazes is still unclear.

HMS was previously found at appreciable concentrations in cloud and fog (Munger et al., 1986; Rao and Collett, 1995), whereas the HMS concentrations observed in atmospheric aerosols in the United States, Germany, and Japan were low (Dixon and Aasen, 1999; Scheinhardt et al., 2014; Suzuki et al., 2001). If HMS does play a role in NCP winter haze, accurate

60 identification and quantification of aerosol HMS are essential. Low oxidant concentrations, high water content, moderate pH, and low temperatures for typical cloud and fog environments together with the presence of SO_2 and formaldehyde (HCHO) favor HMS formation (Deister et al., 1986; Boyce and Hoffmann, 1984; Kok et al., 1986; Lagrange et al., 1999). Such conditions are common during severe winter hazes in the NCP, such as Beijing (Zheng et al., 2015b; Cheng et al., 2016; Rao et al., 2016).

65 In this study, combining aerosol time-of-flight mass spectrometer (ATOFMS) measurement and optimized ion chromatography method, we identified the ubiquity of HMS in Beijing winter and quantified its contribution to severe winter hazes. We

demonstrated that the reaction between HCHO and dissolved SO_2 to form HMS in aerosol water was an important pathway that contributed to winter haze pollution in Beijing, not only contributing a substantial mass of OM but also leading to overestimation of sulfate in conventional measurements. High concentrations of precursors (i.e., SO_2 and HCHO) coupled

70   with appropriate conditions (i.e., low oxidants, low temperature, high relative humidity, and moderately acid pH) in severe winter hazes favored the heterogeneous HMS formation. Furthermore, two-year continuous winter measurements from 2015 to 2016 indicated that HMS concentrations increased with the increase of HCHO. Finally, we discussed the implications of heterogeneous HMS chemistry for haze chemistry and control strategies.

2 Methods

75   ### 2.1 Sampling site

Field measurements were conducted in urban Beijing in 2015 and the winter of 2016. The observational sites are located in Tsinghua University (40.00° N, 116.34° E), the Chinese Academy of Meteorological Sciences (39.95° N, 116.33° E), and the Chinese Research Academy of Environmental Sciences (40.05° N, 116.42° E), respectively (Fig. S1 in the Supplement). Details of the measurements and analysis are described below.

80   ### 2.2 ATOFMS measurement and data analysis

Real-time ATOFMS (model 3800-100, TSI, Inc.) measurement in Beijing was carried out from December 21, 2015 to January 8, 2016. The observation site was on the tenth floor of the School of Environment, Tsinghua University, approximately 35 m above ground level. Details of ATOFMS measurements have been described in previous studies (Furutani et al., 2011). Briefly, ATOFMS simultaneously measures the size and chemical composition of individual particles. The inlet flow rate is $0.1 \, \mathrm{L \, min^{-1}}$.

85   Ambient aerosols between 100 nm and 3000 nm enter the ATOFMS through an aerodynamic focusing lens and are accelerated to their size-dependent terminal velocities. The particle velocity is determined by measuring the time-of-flight between two solid state green lasers ($\lambda = 532$ nm, 50 mW, CL532‑050‑L, CrystaLaser, NV, USA). The particle size is calculated from the measured velocity based on the calibration curve between particle size and velocity. In addition, the velocity is used to trigger the 266 nm Nd:YAG laser (~1 mJ/pulse), which desorbs and ionizes the particle. The generated positive and negative

90   ions are detected using a bipolar reflectron ToF-MS. The ATOFMS aerodynamic sizing was calibrated by standard polystyrene latex spheres (PSL) with different sizes (d = 151, 199, 269, 350, 499, and 799 nm, Duke Scientific Corp., USA). Mass calibration of ATOFMS was conducted with the standard solution (Ba, K, Pb, Na, Li, V in HNO_3).

During the winter campaign, ATOFMS detected 4,495,233 particles containing both size and chemical information, accounting for 49% of all sized particles. Single particle mass spectrometers identify the peak at m/z −111 as HMS (Whiteaker and Prather,

95   2003; Dall'Osto et al., 2009; Neubauer et al., 1997). To eliminate interferences, HMS-containing particles were screened with a relatively high threshold: the peak area at m/z −111 should be greater than 2% of the total integrated area of the single particle

negative ion mass spectrum (Whiteaker and Prather, 2003).

2.3 Offline sample collection and ion chromatography analysis

PM$_{2.5}$ samples were collected on 47 mm quartz filters at a flow rate of 15.4 L min^{-1} for 23.5 hours every day in 2015 and 2016.

100   Here we analyzed some samples during haze episodes in four seasons in 2015 and winter of 2016. In the winter of 2016, we also collected PM$_{2.5}$ samples on 90 mm quartz filters at a flow rate of 100 L min^{-1} in the daytime and nighttime, respectively. The filters were baked in Muffle furnace at 550 °C for 4 h and put in the cassettes and packed using aluminum foil prior to sampling, and all samples were stored at −20 °C before analysis. A quarter of each 47 mm filter or 3.14 cm^2 punch from each 90 mm filter was extracted twice with 5 mL 0.1% HCHO solution, ultrasonic oscillation for 20 min in an ice water bath and

105   then filtered through the 0.45 μm membrane syringe filter. Two extracts were combined for ion chromatography analysis. We found that HMS slowly converted to sulfate during conventional sample preparation (i.e. water extraction), leading to HMS underestimation and sulfate overestimation, and extraction with 0.1% HCHO solution can counteract the HMS decomposition (Fig. S2a, b).

A Dionex Integrion HPIC Ion Chromatography system with AS11-HC analytical column and AG11-HC guard column (Dionex

110   Corp., CA, US), typical columns used in previous studies during winter hazes in Beijing (Cao et al., 2014), was used for the anion analysis. The separation of HMS and sulfate depends on ion chromatography conditions (i.e., column and eluent). We found the separation of HMS and sulfate peak was not good under conventional condition (eluent: 30 mM KOH, flow rate: 1.5 mL min^{-1}) (Fig. S2c). Here we used an eluent of 11 mM KOH (pH≈12) with a flow rate 1.5 mL min^{-1}, and successfully distinguished HMS from sulfate (Fig. S2d). In addition, Moch et al. and Dovrou et al. found that the AS22 column could not

115   fully separate HMS and sulfate, while AS12A was able to successfully separate HMS and sulfate (Moch et al., 2018; Dovrou et al., 2019). Actually, HMS dissociates into SO$_3^{2-}$ and HCHO rapidly in the eluent due to the short characteristic time for HMS dissociation at pH 12, and HMS concentration is measured in the form of sulfite in ion chromatography (Fig. S2e) (Dasgupta, 1982). Thus, ion chromatography method cannot distinguish HMS from sulfite directly. Previous studies indicated that the concentration of sulfite in atmospheric aerosols was much lower than that of HMS (Dixon and Aasen, 1999; Dabek-

120   Zlotorzynska et al., 2002). In order to distinguish between sulfite and HMS, a second analysis was performed using dilute nitric acid (pH≈3) to extract samples. In the second analysis, sulfite is oxidized to sulfate, while HMS is stable. We tested some samples collected during severe winter hazes in Beijing, and found that the influence of sulfite on HMS measurement was negligible (Fig. S2f). The method detection limit was 0.02 mg L^{-1} for SO$_3^{2-}$, equal to 0.03 mg L^{-1} for HMS. The blank quartz filter was analyzed as control. We also tested the accuracy (through recovery analysis) and precision (through repetitive

125   analysis) of the method on HMS analysis. The recovery of blank and sample was 95.6% and 112.5%, respectively. The relative standard deviation (RSD) of triple repetitive analysis of the sample (average: 3.17 mg L^{-1}) was 4.7%.

2.4 Supplementary data and analysis

Online measurements of gaseous pollutants, particulate matter, and meteorological parameters were conducted on the roof of

School of Economics and Management, approximately 20 m above ground level and 100 m away from the ATOFMS
130 observation site, on the campus of Tsinghua University as described in previous works (Xu et al., 2017; Zheng et al., 2015b).
In brief, hourly mass concentrations of $PM_{2.5}$ and PM_1 were monitored based on the β-ray absorption method by using two
dichotomous monitors (PM-712 and PM-714; Kimoto Electric Co., Ltd., Japan). The hourly concentrations of carbonaceous
species including organic carbon (OC) and elemental carbon (EC) in $PM_{2.5}$ in 2015 were monitored by APC-710 (Kimoto
Electric Co., Ltd., Japan). The hourly OC and EC concentrations in $PM_{2.5}$ in 2016 winter were measured by a Sunset Model 4
135 Semi-Continuous Carbon Analyzer (Beaverton, OR, USA). We adopted a factor of 1.6 to convert the OC mass into OM mass
(Xing et al., 2013; Zhang et al., 2017). The hourly concentrations of gaseous pollutants including SO_2, CO, and O_3 were
monitored with MCSAM-13 system (Kimoto Electric, Ltd., Japan). The hourly meteorological parameters including
temperature and relative humidity (RH) were simultaneously monitored with an automatic meteorological observation
instrument (Milos 520, VAISALA Inc., Finland).
140 Online concentrations of water-soluble ions in $PM_{2.5}$ and inorganic gases were measured by the Monitor for AeRosols and
Gases (MARGA, Metrohm Ltd., Switzerland) in 2016 winter at the Chinese Research Academy of Environmental Sciences,
about 9 kilometers from Tsinghua University. We calculated the aerosol water content and pH with the ISORROPIA-II
thermodynamic equilibrium model (Fountoukis and Nenes, 2007). Briefly, we adopted the forward mode constrained by gas
(HNO_3, HCl, and NH_3) + aerosol (SO_4^{2-}, NO_3^-, Cl^-, K^+, Ca^{2+}, Na^+, Mg^{2+}, NH_4^+) measurements, and assumed the aerosol phase
145 state to be metastable (Hennigan et al., 2015). The model inputs were taken from the MARGA measurements.
Online HCHO measurement was conducted at the Chinese Academy of Meteorological Sciences, about 6 kilometers from
Tsinghua University. The HCHO was measured by an Aero-Laser GmbH HCHO analyzer (model AL4021) based on the
Hantzsch reaction, as described in the previous work (Song et al., 2019). The Hantzsch reagents were prepared every 3 days
and stored in a refrigerator. This analyzer was calibrated with a 1 μM HCHO standard solution every 2 to 3 days. The detection
150 limit is 150 ppt in the field, and the accuracy and precision are ±15% or 150 ppt and ±10% or 150 ppt, respectively (Hak et al.,
2005).
The anthropogenic emission inventory data of HCHO was derived from the Multi-resolution Emission Inventory of China
(MEIC) model framework (available at http://www.meicmodel.org/), as described in detail by earlier papers (Li et al., 2019b).
Briefly, the emissions were calculated based on a technology-based methodology using updated activity data from the MEIC
155 model framework and a collection of state-of-the-art emission factors and source profiles. The uncertainty of volatile organic
compounds (VOCs) emission inventory in MEIC was estimated to be ±68% (Cheng et al., 2019).

3 Results and discussion

3.1 Identification of HMS in atmospheric particles

Our field measurements with ATOFMS showed that HMS was ubiquitous in aerosols during Beijing winter. During the winter
160 observation, we found that 76% of particles contained the peak at m/z −111, and screened HMS-containing particles (the

relative peak area at m/z −111 greater than 2%, Fig. 1) accounted for 9% of the total particles. It should be noted that KCl_2^- and methyl sulfate ($CH_3SO_4^-$) could also contribute to the peak at m/z −111. According to the natural isotopic compositions, we considered that the contribution of KCl_2^- was insignificant. The peak area ratio of m/z −111 to m/z −113 in all screened particles was 18.7, which was consistent with the natural isotopic distribution of HMS (18.7) and much larger than that of

165   KCl_2^- (4.8). Also, the peak area ratio of m/z −109 to m/z −111 in all screened particles was 0.03, which was much smaller than that of KCl_2^- (1.4). Considering the moderate aerosol pH (4–5; see Sect. 3.3) in Beijing winter haze and the tendency of m/z −111 to exist in supermicrometer particles (see Sect. 3.2) in this study, the observed peak at m/z −111 was unlikely to be methyl sulfate since methyl sulfate formation requires relatively high acid conditions (Lee, 2003) and organosulfates tend to exist in submicrometer particles (Hatch et al., 2011). Therefore, the peak at m/z −111 in ambient particles was almost entirely assigned

170   to HMS. Ambient particles in Beijing winter contained a large amount of ammonium relative to sodium, and the ammonium was more common than sodium in HMS-containing particles (Fig. S3), indicating that the matrix effects on HMS detection due to counterions was not significant, because ammonium promotes the presence of the HMS marker peak in the negative ion spectrum (Neubauer et al., 1997; Whiteaker and Prather, 2003).

3.2 Quantification of HMS in atmospheric particles

175   Based on the optimized ion chromatography method, we quantified the HMS concentration and its contribution to haze pollution. We found that HMS concentration was appreciable in humid winter haze conditions, but low in clean winter periods, dry winter haze conditions, and other seasons (Fig. S4). HMS concentration exhibited similar periodic variation to that of $PM_{2.5}$ and sulfate concentration in winter, and was consistent with RH variation. With the deterioration of winter haze in 2015, i.e., from clean ($PM_{2.5} \leq 75$ μg m^{-3}), polluted ($75 < PM_{2.5} \leq 150$ μg m^{-3}) to heavily polluted ($PM_{2.5} > 150$ μg m^{-3}), HMS

180   concentration increased rapidly (Fig. 2a). Also, the molar ratio of HMS to sulfate increased from 0 (clean), 0.02 (polluted), to 0.06 (heavily polluted). During the HMS increase process, RH, SO_2, and HCHO concentration increases, while O_3 concentration declines (Fig. 2b, c). HMS tends to exist in supermicrometer particles. During the HMS events, the ratio of $PM_{1-2.5}$ to $PM_{2.5}$ was generally greater than 0.4, indicating the large contribution of supermicrometer aerosols. The size distribution of HMS-containing particles displayed a mode at larger sizes compared with the total particle size distribution, and the

185   percentage of HMS-containing particles increased with particle size and remained relatively constant when the diameter is greater than 1 μm (Fig. 2d), indicating the predominance of HMS in large particles.

Field measurements in Beijing in winter 2016 also showed similar HMS evolution pattern, i.e., high HMS concentrations usually occurred in humid haze conditions with high concentrations of precursors, high RH, and weak photochemical activity (Fig. S5 and S6), but HMS concentrations were higher than in winter 2015. During severe winter hazes ($PM_{2.5} > 150$ μg m^{-3}),

190   HMS accounted for 1.5% (0.4–4%) of $PM_{2.5}$ mass in 2015, and this contribution increased to 2.7% (0.3–6%) in 2016 (Fig. S7). Correspondingly, the contribution of HMS to estimated OM increased from 4.4% (0.9–11%) in 2015 to 7.6% (1.4–15%) in 2016. The increase of HMS from winter 2015 to winter 2016 was consistent with the increasing HCHO concentration. Instead, the concentrations of SO_2 during severe winter hazes decreased significantly due to the strict control measures, resulting in a

decrease of sulfate. Accordingly, the molar ratio of HMS to sulfate increased significantly from winter 2015 to winter 2016.
195 Considering the conversion of HMS to sulfate in conventional ion chromatography analysis, the observed sulfate concentrations during severe winter hazes can be overestimated by 6.4% (3–15%) in 2015, and the ratio increased to 15% (2.5–36%) in 2016.

3.3 Factors influencing HMS formation

HMS is formed in the aqueous phase, such as cloud (Moch et al., 2018), fog (Munger et al., 1986), and aerosol water (Song et
200 al., 2019). We find that HMS is present in aerosols regardless of the presence of cloud/fog (Fig. S8a, b), and HMS concentrations show a good correlation ($r = 0.92$, $P < 0.01$) with aerosol water content (Fig. S8b), indicating that aerosol water serves as a medium for HMS formation. In some HMS events, cloud/fog processes exist (Fig. S8a, b) and may contribute together with heterogeneous processes in aerosol water to the formation of HMS. Our results indicate that high concentrations of precursors (i.e., SO_2 and HCHO) coupled with appropriate conditions (i.e., low oxidants, low temperature, high RH, and
205 moderately acid pH) in severe winter hazes in the NCP facilitate the heterogeneous HMS formation.

Low oxidants and low temperature during winter haze facilitate the HMS formation. The S(IV) oxidation reactions are major competitions with HMS formation (Pandis and Seinfeld, 1989). The low O_3 concentration and low solar radiation during HMS events (Fig. S4 and S5) indicate the weak photochemical activity. Previous measurements also showed that OH radical and H_2O_2 concentrations were low in winter, especially during severe winter hazes (Tan et al., 2018; Zhang et al., 2012; Ye et al.,
210 2018). Low temperature increases the solubility of gas (Sander, 2015), whereas decreases the reaction rate constant for HMS production (Boyce and Hoffmann, 1984). According to the kinetics calculation (Song et al., 2019), the increase of gas solubility in water at low temperature is greater than the decrease of reaction rate constant, leading to higher HMS formation rate in winter hazes. Once formed, HMS is relatively stable due to the self-acidification and resistance to oxidation by O_3, H_2O_2, and O_2 (Hoigne et al., 1985; Kok et al., 1986; Munger et al., 1986; Dasgupta et al., 1980).

215 High RH is a key factor driving fast HMS formation in winter hazes. The HMS concentration increases slowly under low RH, whereas it increases rapidly under high RH (Fig. S9). Similarly, the aerosol water content exhibits an exponential increase with RH (Fig. S10), providing abundant reaction interfaces for HMS formation. HMS concentration started to increase significantly with the enhancement in RH when the RH > 60%, coinciding with the reported deliquesce RH of particles in Beijing winter (Liu et al., 2017b). With the increase of RH, atmospheric sulfur distribution shifts toward particle phase and more particulate
220 sulfur exist in the form of HMS (Fig. 3). The molar ratio of HMS to sulfate also started to increase rapidly at the RH ~60%, and high values usually occurred under severe winter hazes with high $PM_{2.5}$ and HMS concentrations.

Moderately acid pH in Beijing winter hazes favors the HMS formation. Previous studies indicated that both HMS formation and decomposition rate increased rapidly with pH, thereby high HMS concentrations were usually observed in moderate pH conditions, since low pH retards the formation of HMS, while high pH is not suitable for its preservation (Munger et al., 1986).
225 The calculation based on the ISORROPIA-II thermodynamic equilibrium model constrained by in situ gas and aerosol measurements showed an average pH value of 4.5 (from 4 to 5) for aerosol water under severe winter hazes in 2016, which

agreed reasonably with previous studies in the NCP (Liu et al., 2017a; Song et al., 2018; Ding et al., 2019; Li et al., 2019a) and was higher than those in the United States and Europe (Bougiatioti et al., 2016; Weber et al., 2016). Under such conditions, the HMS formation is favored, whereas the decomposition of HMS is negligible, thereby resulting in the observed high HMS

230   concentrations during severe winter hazes.

3.4 Implications for haze chemistry and control strategies

Our findings reveal the significant contribution of HMS to severe winter hazes. We propose a more comprehensive conceptual model of heterogeneous sulfur chemistry in NCP haze events, including traditional sulfate formation, and HMS formation under high HCHO concentration, low oxidants, low temperature, high RH, and moderate pH (Fig. 4a). With the deterioration

235   of winter haze, atmospheric oxidation capacity decreases associated with the weak photochemistry activity, while heterogeneous HMS chemistry is enhanced, resulting in the increase of HMS concentration and the ratio of HMS to sulfate (Fig. 4b). Adding heterogeneous HMS chemistry into the model could improve the simulation of OM. In addition, the presence of HMS could lead to sulfate overestimation in conventional measurements, such as ion chromatography and aerosol mass spectrometry (Song et al., 2019). This can partly explain the discrepancy between sulfate simulation and observation during

240   severe NCP winter hazes. Furthermore, HMS can be used as a tracer for heterogeneous chemistry and moderate pH during typical winter haze pollution.

Our results suggest that the reduction in HCHO concentration can help to mitigate severe winter haze pollution in the NCP. Previous studies show that HCHO is an important source of RO_x (OH+HO_2+RO_2) radicals and ozone (Tan et al., 2018; Li et al., 2019b; Niu et al., 2016), and has high toxicity as a Group 1 human carcinogen (Niu et al., 2016), here we further

245   demonstrate its significant contribution to particulate matter in winter. Since the implementation of 'Air Pollution Prevention and Control Action Plan' in 2013, SO_2 concentrations during winter hazes in Beijing have decreased significantly due to the implementation of desulfurization measures and controls on emission activities (Zheng et al., 2015b; Zheng et al., 2018), resulting in the decrease of sulfate, while HCHO concentrations show an increasing trend (Fig. S7), leading to the increased importance of HMS in winter haze. HCHO comes from primary emission and secondary formation (Chen et al., 2014; Sheng

250   et al., 2018). Therefore, the cooperative emission reduction in primary HCHO, which mainly comes from residential solid fuel (biofuel and coal) combustion and transportation (Fig. S11) (Li et al., 2019b), and VOCs (e.g., alkenes, aromatics, and alkanes) related to secondary HCHO formation should be considered in the future pollutant control strategies in the NCP. Furthermore, the HMS chemistry and related control strategies can be applicable to other regions with high SO_2 and HCHO concentrations, such as India (De Smedt et al., 2015; Li et al., 2017).

255   ### 4 Conclusion

Combining field measurements and laboratory experiments, we show the ubiquity of HMS in aerosols and the quantification of the large amounts of HMS in PM_{2.5} in Beijing winter, and elucidate the heterogeneous HMS chemistry in winter haze. High

concentrations of precursors (SO_2 and HCHO), low oxidant levels, low temperature, high RH, and moderately acid pH during severe winter hazes facilitate the heterogeneous formation of HMS, which could account for up to 15% of OM in winter haze and lead to 36% overestimates of sulfate. The HMS concentration and the molar ratio of HMS to sulfate increased with the deterioration of winter haze, as well as from winter 2015 to winter 2016 with the growth of HCHO concentration. Our results reveal the significant contribution of HMS to severe winter hazes, which help to improve the prediction of OM and sulfate, and suggest that the reduction in HCHO can help to mitigate severe winter haze pollution.

Data availability. All data that support the findings of this study are available in this article and its Supplement or from the corresponding author on request.

Author contributions. TM, FD, and KH designed research; TM, HF, FD, TK, JJ, YM, LZ, TH, MT, and KH performed research; TM, HF, TK, and SS contributed new reagents/analytic tools; TM and HF analyzed data; QZ, GG, and ML provided emission inventory; XX and YW provided formaldehyde data; JG and JW provided MARGA data; TM wrote the paper; and TM, HF, FD, JJ, QZ, and KH revised the paper.

Competing interests. The authors declare that they have no conflict of interest.

Acknowledgements. This work was supported by the National Science and Technology Program of China (2017YFC0211601), the National Natural Science Foundation of China (81571130090), and National Research Program for Key Issues in Air Pollution Control (DQGG0103). We thank Weiya Yu and Xiaodong Liu for helpful discussions.

References

Bougiatioti, A., Nikolaou, P., Stavroulas, I., Kouvarakis, G., Weber, R., Nenes, A., Kanakidou, M., and Mihalopoulos, N.: Particle water and pH in the eastern Mediterranean: source variability and implications for nutrient availability, Atmos. Chem. Phys., 16, 4579–4591, https://doi.org/10.5194/acp-16-4579-2016, 2016.

Boyce, S. D., and Hoffmann, M. R.: Kinetics and mechanism of the formation of hydroxymethanesulfonic acid at low pH, J. Phys. Chem., 88, 4740–4746, https://doi.org/10.1021/j150664a059, 1984.

Cao, C., Jiang, W. J., Wang, B. Y., Fang, J. H., Lang, J. D., Tian, G., Jiang, J. K., and Zhu, T. F.: Inhalable Microorganisms in Beijing's $PM_{2.5}$ and PM_{10} Pollutants during a Severe Smog Event, Environ. Sci. Technol., 48, 1499–1507, https://doi.org/10.1021/es4048472, 2014.

Chen, W. T., Shao, M., Lu, S. H., Wang, M., Zeng, L. M., Yuan, B., and Liu, Y.: Understanding primary and secondary sources of ambient carbonyl compounds in Beijing using the PMF model, Atmos. Chem. Phys., 14, 3047–3062, https://doi.org/10.5194/acp-14-3047-2014, 2014.

Chen, Y., Xu, L., Humphry, T., Hettiyadura, A. P. S., Ovadnevaite, J., Huang, S., Poulain, L., Schroder, J. C., Campuzano-Jost, P., Jimenez, J. L., Herrmann, H., O'Dowd, C., Stone, E. A., and Ng, N. L.: Response of the Aerodyne Aerosol Mass Spectrometer to Inorganic Sulfates and Organosulfur Compounds: Applications in Field and Laboratory Measurements,

290   Environ. Sci. Technol., 53, 5176–5186, https://doi.org/10.1021/acs.est.9b00884, 2019.

Cheng, J., Su, J., Cui, T., Li, X., Dong, X., Sun, F., Yang, Y., Tong, D., Zheng, Y., Li, Y., Li, J., Zhang, Q., and He, K.: Dominant role of emission reduction in PM$_{2.5}$ air quality improvement in Beijing during 2013–2017: a model-based decomposition analysis, Atmos. Chem. Phys., 19, 6125–6146, https://doi.org/10.5194/acp-19-6125-2019, 2019.

Cheng, Y. F., Zheng, G. J., Wei, C., Mu, Q., Zheng, B., Wang, Z. B., Gao, M., Zhang, Q., He, K. B., Carmichael, G., Poschl,
295   U., and Su, H.: Reactive nitrogen chemistry in aerosol water as a source of sulfate during haze events in China, Sci. Adv., 2, e1601530, https://doi.org/10.1126/sciadv.1601530, 2016.

Dabek-Zlotorzynska, E., Piechowski, M., Keppel-Jones, K., and Aranda-Rodriguez, R.: Determination of hydroxymethanesulfonic acid in environmental samples by capillary electrophoresis, J. Sep. Sci., 25, 1123–1128, https://doi.org/10.1002/1615-9314(20021101)25:15/17<1123::aid-jssc1123>3.0.co;2-3, 2002.

300   Dall'Osto, M., Harrison, R. M., Coe, H., and Williams, P.: Real-time secondary aerosol formation during a fog event in London, Atmos. Chem. Phys., 9, 2459–2469, https://doi.org/10.5194/acp-9-2459-2009, 2009.

Dasgupta, P. K., Decesare, K., and Ullrey, J. C.: Determination of atmospheric sulfur-dioxide without tetrachloromercurate (II) and the mechanism of the schiff reaction, Anal. Chem., 52, 1912–1922, https://doi.org/10.1021/ac50062a031, 1980.

Dasgupta, P. K.: On the ion chromatographic determination of S(IV), Atmos. Environ., 16, 1265–1268,
305   https://doi.org/10.1016/0004-6981(82)90217-7, 1982.

De Smedt, I., Stavrakou, T., Hendrick, F., Danckaert, T., Vlemmix, T., Pinardi, G., Theys, N., Lerot, C., Gielen, C., Vigouroux, C., Hermans, C., Fayt, C., Veefkind, P., Müller, J. F., and Van Roozendael, M.: Diurnal, seasonal and long-term variations of global formaldehyde columns inferred from combined OMI and GOME-2 observations, Atmos. Chem. Phys., 15, 12519–12545, https://doi.org/10.5194/acp-15-12519-2015, 2015.

310   Deister, U., Neeb, R., Helas, G., and Warneck, P.: Temperature Dependence of the Equilibrium CH$_2$(OH)$_2$ + HSO$_3^-$ = CH$_2$(OH)SO$_3^-$ + H$_2$O in Aqueous Solution, J. Phys. Chem., 90, 3213–3217, https://doi.org/10.1021/j100405a033, 1986.

Ding, J., Zhao, P., Su, J., Dong, Q., Du, X., and Zhang, Y.: Aerosol pH and its driving factors in Beijing, Atmos. Chem. Phys., 19, 7939–7954, https://doi.org/10.5194/acp-19-7939-2019, 2019.

Dixon, R. W., and Aasen, H.: Measurement of hydroxymethanesulfonate in atmospheric aerosols, Atmos. Environ., 33, 2023–
315   2029, https://doi.org/10.1016/s1352-2310(98)00416-6, 1999.

Dovrou, E., Lim, C. Y., Canagaratna, M. R., Kroll, J. H., Worsnop, D. R., and Keutsch, F. N.: Measurement techniques for identifying and quantifying hydroxymethanesulfonate (HMS) in an aqueous matrix and particulate matter using aerosol mass spectrometry and ion chromatography, Atmos. Meas. Tech., 12, 5303–5315, https://doi.org/10.5194/amt-12-5303-2019, 2019.

Fountoukis, C., and Nenes, A.: ISORROPIA II: a computationally efficient thermodynamic equilibrium model for K$^+$-Ca^{2+}-
320   Mg^{2+}-NH$_4^+$-Na$^+$-SO$_4^{2-}$-NO$_3^-$-Cl$^-$-H$_2$O aerosols, Atmos. Chem. Phys., 7, 4639–4659, https://doi.org/10.5194/acp-7-4639-2007, 2007.

Furutani, H., Jung, J., Miura, K., Takami, A., Kato, S., Kajii, Y., and Uematsu, M.: Single-particle chemical characterization and source apportionment of iron-containing atmospheric aerosols in Asian outflow, J. Geophys. Res. Atmos., 116, D18204,

https://doi.org/10.1029/2011jd015867, 2011.

325 Hak, C., Pundt, I., Trick, S., Kern, C., Platt, U., Dommen, J., Ordonez, C., Prevot, A. S. H., Junkermann, W., Astorga-Llorens, C., Larsen, B. R., Mellqvist, J., Strandberg, A., Yu, Y., Galle, B., Kleffmann, J., Lorzer, J. C., Braathen, G. O., and Volkamer, R.: Intercomparison of four different in-situ techniques for ambient formaldehyde measurements in urban air, Atmos. Chem. Phys., 5, 2881–2900, https://doi.org/10.5194/acp-5-2881-2005, 2005.

Hatch, L. E., Creamean, J. M., Ault, A. P., Surratt, J. D., Chan, M. N., Seinfeld, J. H., Edgerton, E. S., Su, Y. X., and Prather,
330 K. A.: Measurements of Isoprene-Derived Organosulfates in Ambient Aerosols by Aerosol Time-of-Flight Mass Spectrometry - Part 1: Single Particle Atmospheric Observations in Atlanta, Environ. Sci. Technol., 45, 5105–5111, https://doi.org/10.1021/es103944a, 2011.

Hennigan, C. J., Izumi, J., Sullivan, A. P., Weber, R. J., and Nenes, A.: A critical evaluation of proxy methods used to estimate the acidity of atmospheric particles, Atmos. Chem. Phys., 15, 2775–2790, https://doi.org/10.5194/acp-15-2775-2015, 2015.

335 Hoigne, J., Bader, H., Haag, W. R., and Staehelin, J.: Rate constants of reactions of ozone with organic and inorganic-compounds in water .3. inorganic-compounds and radicals, Water Res., 19, 993–1004, https://doi.org/10.1016/0043-1354(85)90368-9, 1985.

Hu, J. L., Wang, P., Ying, Q., Zhang, H. L., Chen, J. J., Ge, X. L., Li, X. H., Jiang, J. K., Wang, S. X., Zhang, J., Zhao, Y., and Zhang, Y. Y.: Modeling biogenic and anthropogenic secondary organic aerosol in China, Atmos. Chem. Phys., 17, 77–92,
340 https://doi.org/10.5194/acp-17-77-2017, 2017.

Huang, R. J., Zhang, Y., Bozzetti, C., Ho, K. F., Cao, J. J., Han, Y., Daellenbach, K. R., Slowik, J. G., Platt, S. M., and Canonaco, F.: High secondary aerosol contribution to particulate pollution during haze events in China, Nature, 514, 218–222, https://doi.org/10.1038/nature13774, 2014.

Kok, G. L., Gitlin, S. N., and Lazrus, A. L.: Kinetics of the formation and decomposition of hydroxymethanesulfonate, J.
345 Geophys. Res. Atmos., 91, 2801–2804, https://doi.org/10.1029/JD091iD02p02801, 1986.

Lagrange, J., Wenger, G., and Lagrange, P.: Kinetic study of HMSA formation and decomposition: Tropospheric relevance, J. Chim. Phys. Phys.- Chim. Biol., 96, 610–633, https://doi.org/10.1051/jcp:1999161, 1999.

Lee, S. H.: Nitrate and oxidized organic ions in single particle mass spectra during the 1999 Atlanta Supersite Project, J. Geophys. Res., 108, D78417, https://doi.org/10.1029/2001jd001455, 2003.

350 Lelieveld, J., Evans, J. S., Fnais, M., Giannadaki, D., and Pozzer, A.: The contribution of outdoor air pollution sources to premature mortality on a global scale, Nature, 525, 367–371, https://doi.org/10.1038/nature15371, 2015.

Li, C., McLinden, C., Fioletov, V., Krotkov, N., Carn, S., Joiner, J., Streets, D., He, H., Ren, X., Li, Z., and Dickerson, R. R.: India Is Overtaking China as the World's Largest Emitter of Anthropogenic Sulfur Dioxide, Sci. Rep., 7, 14304, https://doi.org/10.1038/s41598-017-14639-8, 2017.

355 Li, H., Cheng, J., Zhang, Q., Zheng, B., Zhang, Y., Zheng, G., and He, K.: Rapid transition in winter aerosol composition in Beijing from 2014 to 2017: response to clean air actions, Atmos. Chem. Phys., 19, 11485–11499, https://doi.org/10.5194/acp-19-11485-2019, 2019a.

Li, M., Zhang, Q., Zheng, B., Tong, D., Lei, Y., Liu, F., Hong, C., Kang, S., Yan, L., Zhang, Y., Bo, Y., Su, H., Cheng, Y., and He, K.: Persistent growth of anthropogenic non-methane volatile organic compound (NMVOC) emissions in China during 1990-2017: drivers, speciation and ozone formation potential, Atmos. Chem. Phys., 19, 8897–8913, https://doi.org/10.5194/acp-2019-125, 2019b.

Liu, M., Song, Y., Zhou, T., Xu, Z., Yan, C., Zheng, M., Wu, Z., Hu, M., Wu, Y., and Zhu, T.: Fine particle pH during severe haze episodes in northern China, Geophys. Res. Lett., 44, 5213–5221, https://doi.org/10.1002/2017gl073210, 2017a.

Liu, Y., Wu, Z., Wang, Y., Xiao, Y., Gu, F., Zheng, J., Tan, T., Shang, D., Wu, Y., Zeng, L., Hu, M., Bateman, A. P., and Martin, S. T.: Submicrometer Particles Are in the Liquid State during Heavy Haze Episodes in the Urban Atmosphere of Beijing, China, Environ. Sci. Tech. Lett., 4, 427–432, https://doi.org/10.1021/acs.estlett.7b00352, 2017b.

Moch, J. M., Dovrou, E., Mickley, L. J., Keutsch, F. N., Cheng, Y., Jacob, D. J., Jiang, J., Li, M., Munger, J. W., Qiao, X., and Zhang, Q.: Contribution of hydroxymethane sulfonate to ambient particulate matter: A potential explanation for high particulate sulfur during severe winter haze in Beijing, Geophys. Res. Lett., 45, 11969–11979, https://doi.org/10.1029/2018gl079309, 2018.

Munger, J. W., Tiller, C., and Hoffmann, M. R.: Identification of hydroxymethanesulfonate in fog water, Science, 231, 247–249, https://doi.org/10.1126/science.231.4735.247, 1986.

Neubauer, K. R., Johnston, M. V., and Wexler, A. S.: On-line analysis of aqueous aerosols by laser desorption ionization, Int. J. Mass Spectrom. Ion Processes, 163, 29–37, https://doi.org/10.1016/s0168-1176(96)04534-x, 1997.

Niu, H., Mo, Z. W., Shao, M., Lu, S. H., and Xie, S. D.: Screening the emission sources of volatile organic compounds (VOCs) in China by multi-effects evaluation, Front. Environ. Sci. Eng., 10, 11, https://doi.org/10.1007/s11783-016-0828-z, 2016.

Pandis, S. N., and Seinfeld, J. H.: Sensitivity analysis of a chemical mechanism for aqueous-phase atmospheric chemistry, J. Geophys. Res. Atmos., 94, 1105–1126, https://doi.org/10.1029/JD094iD01p01105, 1989.

Rao, X., and Collett, J. L.: Behavior of S(IV) and formaldehyde in a chemically heterogeneous cloud, Environ. Sci. Technol., 29, 1023–1031, https://doi.org/10.1021/es00004a024, 1995.

Rao, Z. H., Chen, Z. M., Liang, H., Huang, L. B., and Huang, D.: Carbonyl compounds over urban Beijing: Concentrations on haze and non-haze days and effects on radical chemistry, Atmos. Environ., 124, 207–216, https://doi.org/10.1016/j.atmosenv.2015.06.050, 2016.

Sander, R.: Compilation of Henry's law constants (version 4.0) for water as solvent, Atmos. Chem. Phys., 15, 4399–4981, https://doi.org/10.5194/acp-15-4399-2015, 2015.

Scheinhardt, S., van Pinxteren, D., Muller, K., Spindler, G., and Herrmann, H.: Hydroxymethanesulfonic acid in size-segregated aerosol particles at nine sites in Germany, Atmos. Chem. Phys., 14, 4531–4538, https://doi.org/10.5194/acp-14-4531-2014, 2014.

Sheng, J., Zhao, D., Ding, D., Li, X., Huang, M., Gao, Y., Quan, J., and Zhang, Q.: Characterizing the level, photochemical reactivity, emission, and source contribution of the volatile organic compounds based on PTR-TOF-MS during winter haze period in Beijing, China, Atmos. Res., 212, 54–63, https://doi.org/10.1016/j.atmosres.2018.05.005, 2018.

Song, S., Gao, M., Xu, W., Sun, Y., Worsnop, D. R., Jayne, J. T., Zhang, Y., Zhu, L., Li, M., Zhou, Z., Cheng, C., Lv, Y., Wang, Y., Peng, W., Xu, X., Lin, N., Wang, Y., Wang, S., Munger, J. W., Jacob, D. J., and McElroy, M. B.: Possible heterogeneous chemistry of hydroxymethanesulfonate (HMS) in northern China winter haze, Atmos. Chem. Phys., 19, 1357–1371, https://doi.org/10.5194/acp-19-1357-2019, 2019.

Song, S. J., Gao, M., Xu, W. Q., Shao, J. Y., Shi, G. L., Wang, S. X., Wang, Y. X., Sun, Y. L., and McElroy, M. B.: Fine-particle pH for Beijing winter haze as inferred from different thermodynamic equilibrium models, Atmos. Chem. Phys., 18, 7423–7438, https://doi.org/10.5194/acp-18-7423-2018, 2018.

Suzuki, Y., Kawakami, M., and Akasaka, K.: H-1 NMR application for characterizing water-soluble organic compounds in urban atmospheric particles, Environ. Sci. Technol., 35, 2656–2664, https://doi.org/10.1021/es001861a, 2001.

Tan, Z. F., Rohrer, F., Lu, K. D., Ma, X. F., Bohn, B., Broch, S., Dong, H. B., Fuchs, H., Gkatzelis, G. I., Hofzumahaus, A., Holland, F., Li, X., Liu, Y., Liu, Y. H., Novelli, A., Shao, M., Wang, H. C., Wu, Y. S., Zeng, L. M., Hu, M., Kiendler-Scharr, A., Wahner, A., and Zhang, Y. H.: Wintertime photochemistry in Beijing: observations of ROx radical concentrations in the North China Plain during the BEST-ONE campaign, Atmos. Chem. Phys., 18, 12391–12411, https://doi.org/10.5194/acp-18-12391-2018, 2018.

Wang, G. H., Zhang, R. Y., Gomez, M. E., Yang, L. X., Zamora, M. L., Hu, M., Lin, Y., Peng, J. F., Guo, S., Meng, J. J., Li, J. J., Cheng, C. L., Hu, T. F., Ren, Y. Q., Wang, Y. S., Gao, J., Cao, J. J., An, Z. S., Zhou, W. J., Li, G. H., Wang, J. Y., Tian, P. F., Marrero-Ortiz, W., Secrest, J., Du, Z. F., Zheng, J., Shang, D. J., Zeng, L. M., Shao, M., Wang, W. G., Huang, Y., Wang, Y., Zhu, Y. J., Li, Y. X., Hu, J. X., Pan, B., Cai, L., Cheng, Y. T., Ji, Y. M., Zhang, F., Rosenfeld, D., Liss, P. S., Duce, R. A., Kolb, C. E., and Molina, M. J.: Persistent sulfate formation from London Fog to Chinese haze, Proc. Natl. Acad. Sci. U. S. A., 113, 13630–13635, https://doi.org/10.1073/pnas.1616540113, 2016.

Wang, Y., Zhang, Q., Jiang, J., Zhou, W., Wang, B., He, K., Duan, F., Zhang, Q., Philip, S., and Xie, Y.: Enhanced sulfate formation during China's severe winter haze episode in January 2013 missing from current models, J. Geophys. Res. Atmos., 119, 10425–10440, https://doi.org/10.1002/2013JD021426, 2014.

Weber, R. J., Guo, H., Russell, A. G., and Nenes, A.: High aerosol acidity despite declining atmospheric sulfate concentrations over the past 15 years, Nat. Geosci., 9, 282–285, https://doi.org/10.1038/ngeo2665, 2016.

Whiteaker, J. R., and Prather, K. A.: Hydroxymethanesulfonate as a tracer for fog processing of individual aerosol particles, Atmos. Environ., 37, 1033–1043, https://doi.org/10.1016/s1352-2310(02)01029-4, 2003.

Xing, L., Fu, T. M., Cao, J. J., Lee, S. C., Wang, G. H., Ho, K. F., Cheng, M. C., You, C. F., and Wang, T. J.: Seasonal and spatial variability of the OM/OC mass ratios and high regional correlation between oxalic acid and zinc in Chinese urban organic aerosols, Atmos. Chem. Phys., 13, 4307–4318, https://doi.org/10.5194/acp-13-4307-2013, 2013.

Xu, L. L., Duan, F. K., He, K. B., Ma, Y. L., Zhu, L. D., Zheng, Y. X., Huang, T., Kimoto, T., Ma, T., Li, H., Ye, S. Q., Yang, S., Sun, Z. L., and Xu, B. Y.: Characteristics of the secondary water-soluble ions in a typical autumn haze in Beijing, Environ. Pollut., 227, 296–305, https://doi.org/10.1016/j.envpol.2017.04.076, 2017.

Yang, W., Li, J., Wang, M., Sun, Y., and Wang, Z.: A Case Study of Investigating Secondary Organic Aerosol Formation

Pathways in Beijing using an Observation-based SOA Box Model, Aerosol Air Qual. Res., 18, 1606–1616, https://doi.org/10.4209/aaqr.2017.10.0415, 2018.

Ye, C., Liu, P., Ma, Z., Xue, C., Zhang, C., Zhang, Y., Liu, J., Liu, C., Sun, X., and Mu, Y.: High H_2O_2 Concentrations Observed during Haze Periods during the Winter in Beijing: Importance of H_2O_2 Oxidation in Sulfate Formation, Environ. Sci. Tech.
430   Lett., 5, 757–763, https://doi.org/10.1021/acs.estlett.8b00579, 2018.

Zhang, X., He, S. Z., Chen, Z. M., Zhao, Y., and Hua, W.: Methyl hydroperoxide (CH_3OOH) in urban, suburban and rural atmosphere: ambient concentration, budget, and contribution to the atmospheric oxidizing capacity, Atmos. Chem. Phys., 12, 8951–8962, https://doi.org/10.5194/acp-12-8951-2012, 2012.

Zhang, Y. J., Cai, J., Wang, S. X., He, K. B., and Zheng, M.: Review of receptor-based source apportionment research of fine
435   particulate   matter   and   its   challenges   in   China,   Sci.   Total   Environ.,   586,   917–929, https://doi.org/10.1016/j.scitotenv.2017.02.071, 2017.

Zhao, B., Wang, S., Donahue, N. M., Jathar, S. H., Huang, X., Wu, W., Hao, J., and Robinson, A. L.: Quantifying the effect of organic aerosol aging and intermediate-volatility emissions on regional-scale aerosol pollution in China, Sci. Rep., 6, 28815, https://doi.org/10.1038/srep28815, 2016.

440   Zheng, B., Zhang, Q., Zhang, Y., He, K. B., Wang, K., Zheng, G. J., Duan, F. K., Ma, Y. L., and Kimoto, T.: Heterogeneous chemistry: a mechanism missing in current models to explain secondary inorganic aerosol formation during the January 2013 haze episode in North China, Atmos. Chem. Phys., 15, 2031–2049, https://doi.org/10.5194/acp-15-2031-2015, 2015a.

Zheng, B., Tong, D., Li, M., Liu, F., Hong, C., Geng, G., Li, H., Li, X., Peng, L., Qi, J., Yan, L., Zhang, Y., Zhao, H., Zheng, Y., He, K., and Zhang, Q.: Trends in China's anthropogenic emissions since 2010 as the consequence of clean air actions,
445   Atmos. Chem. Phys., 18, 14095–14111, https://doi.org/10.5194/acp-18-14095-2018, 2018.

Zheng, G. J., Duan, F. K., Su, H., Ma, Y. L., Cheng, Y., Zheng, B., Zhang, Q., Huang, T., Kimoto, T., Chang, D., Pöschl, U., Cheng, Y. F., and He, K. B.: Exploring the severe winter haze in Beijing: the impact of synoptic weather, regional transport and heterogeneous reactions, Atmos. Chem. Phys., 15, 2969–2983, https://doi.org/10.5194/acp-15-2969-2015, 2015b.
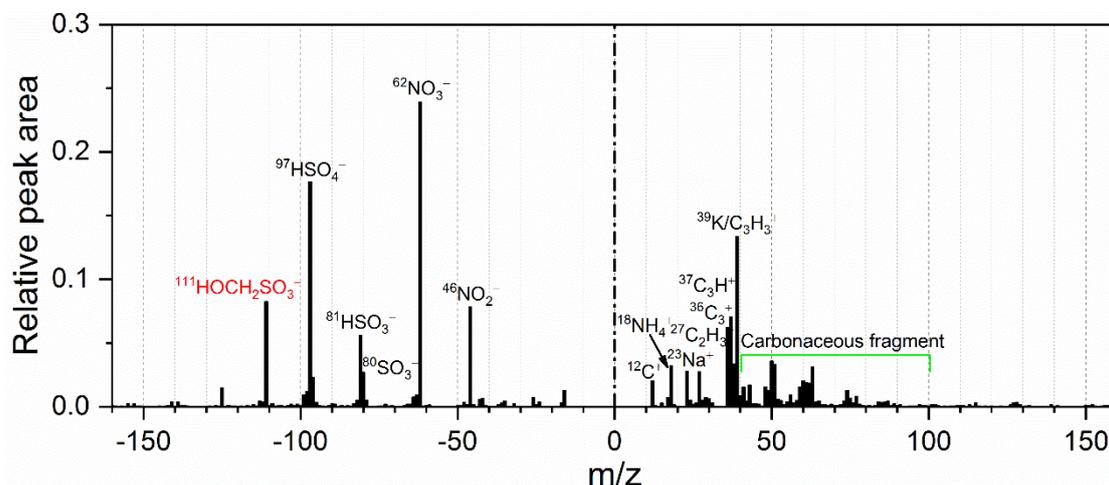
450   **Figure 1.** Presence of HMS in single particle mass spectra during winter in Beijing. The peak at *m/z* −111 is attributed to HMS ($HOCH_2SO_3^-$). The peaks at *m/z* −80 (SO_3^-), −81 (HSO_3^-), −97 (HSO_4^-), −46 (NO_2^-), and −62 (NO_3^-) are also common in the negative ion spectrum, indicating the presence of sulfur species and nitrate. In the positive mass spectra, inorganic ions (*m/z* 18 NH_4^+, 23 Na^+, and 39 K^+), elemental carbon (*m/z* 12 C^+, 36 C_3^+, and 48 C_4^+), and organic carbon (*m/z* 27 $C_2H_3^+$, 37 C_3H^+, 39 $C_3H_3^+$, and 43 $C_2H_3O^+$) are present.
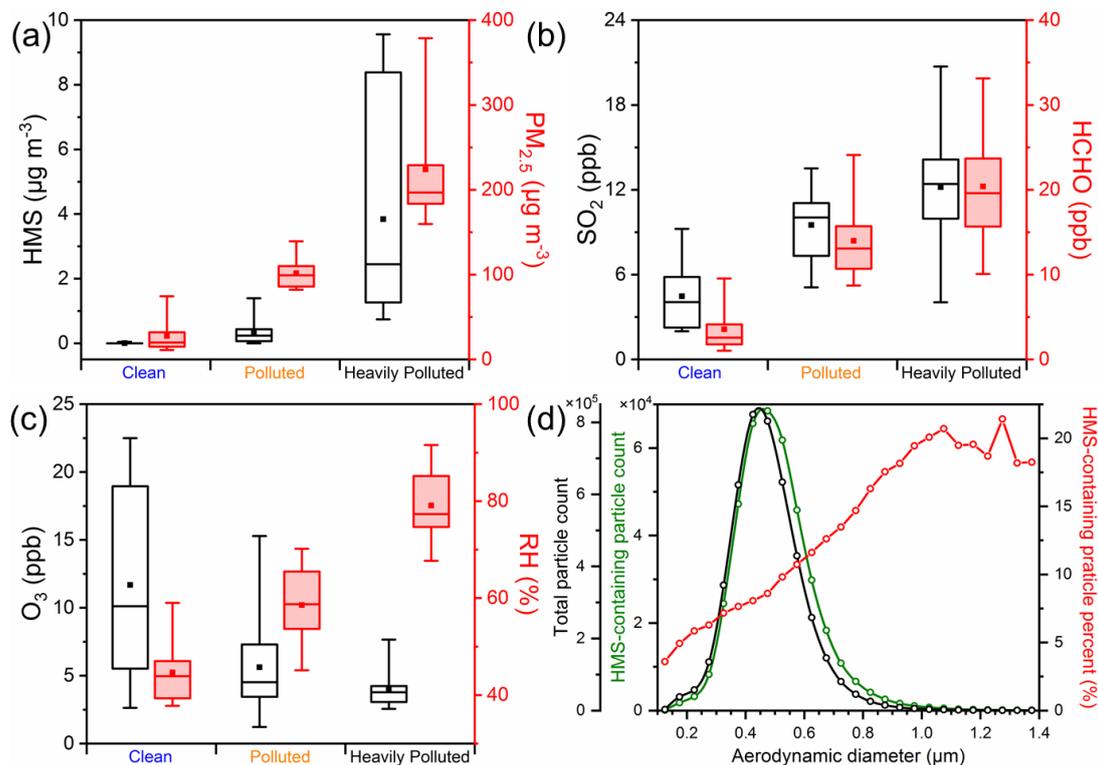
455

Figure 2. Evolution of HMS in Beijing winter of 2015. **(a-c)** Concentrations of HMS, $PM_{2.5}$, SO_2, HCHO, and O_3, and RH at

different pollution levels from 26 November 2015 to 8 January 2016. In the box-whisker plots, the whiskers, boxes, and points indicate the 95th, 75th, 50th, 25th, 5th percentiles and mean values, respectively. **(d)** Size distribution of HMS-containing particles from 21 December 2015 to 8 January 2016.
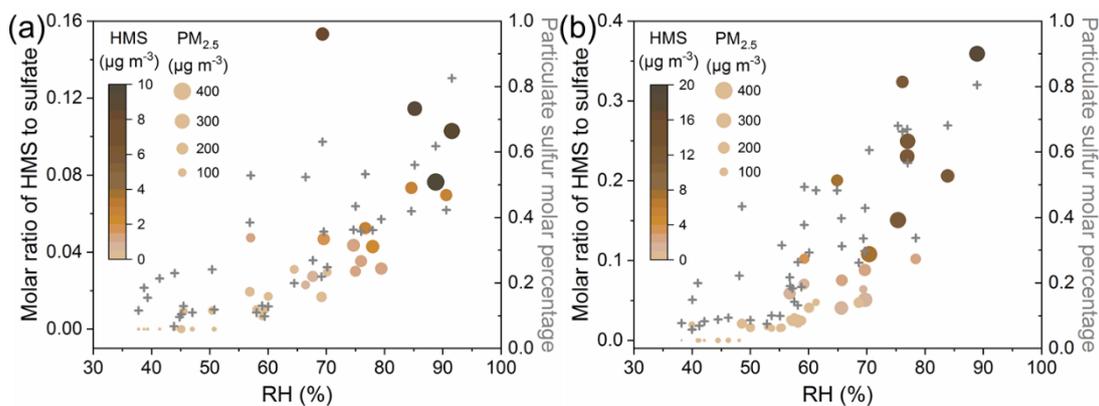
460

Figure 3. Evolution of sulfur distribution with the increase of RH in the winter of 2015 and 2016. **(a)** Relationship between the molar ratio of HMS to sulfate, particulate sulfur molar percentage, and RH in winter 2015. The circles represent the molar ratio of HMS to sulfate colored by HMS concentrations, and the sizes of the circles are scaled to the $PM_{2.5}$ mass concentrations. The gray crosses represent the particulate sulfur molar percentage. Particulate sulfur molar percentage =

465 $\frac{n(SO_4^{2-})+n(HMS)}{n(SO_4^{2-})+n(HMS)+n(SO_2)}$. **(b)** Relationship between the molar ratio of HMS to sulfate, particulate sulfur molar percentage, and RH in winter 2016.
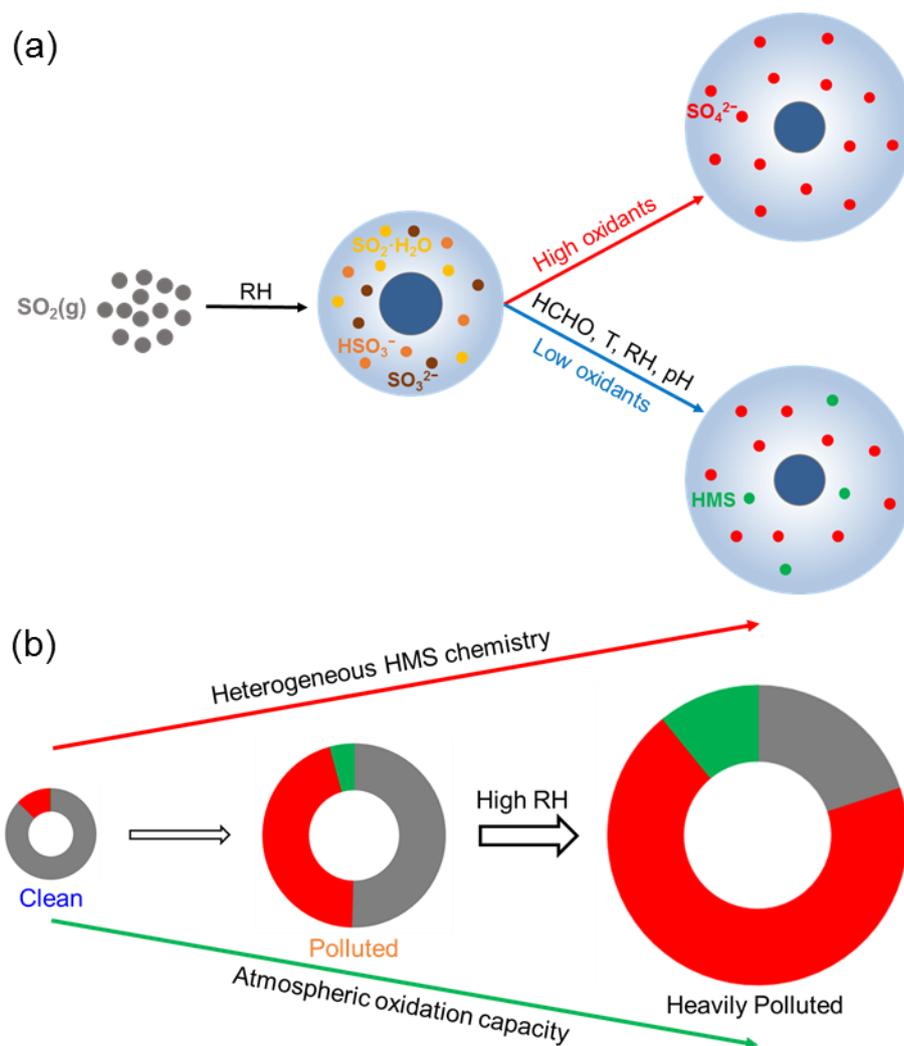
Figure 4. Schematic of the heterogeneous sulfur chemistry. **(a)** Oxidation and addition reaction pathways of dissolved SO_2 in aerosol water under different atmospheric conditions. **(b)** Evolution of sulfur-containing species during winter haze deterioration in the NCP. With the increase of RH and decrease of atmospheric oxidation capacity under NCP winter hazes, atmospheric sulfur distribution shifts toward particle phase and more particulate sulfur exists in the form of HMS. The gray, red, and green colors represent SO_2, SO_4^{2-} and HMS, respectively.